

# Electromagnetic Force and Deformation in Transformer Winding

Arul Sathya M

Department of Electrical and Electronics Engineering,  
Velammal Institute of Technology,  
Panchetti, Tamil Nadu, India.

Usa Savadamuthu

Division of High Voltage Engineering  
College of Engineering, Guindy,  
Anna University, Chennai, Tamil Nadu, India.

## Abstract

Power transformer is one of the major and key apparatus in electric power system. Monitoring and diagnosis of transformer fault are necessary for improving the life period of transformer. Under short circuit conditions, due to excessive forces the transformer windings get deformed resulting in mechanical and electrical changes. If these forces are not properly restrained, major failures are likely to occur. In the present work, computation and analysis of electromagnetic force distribution and resulting displacement/deformation are carried out for two cases from literature using Finite Element method (FEM) based field solvers.

**Keywords:** Transformer winding, Finite element method, Force distribution, Deformation

## I. INTRODUCTION

Transformers are subjected to a variety of electrical, mechanical and thermal stresses during normal life time and they fail when these stresses exceed the threshold levels. One of the major concerns for transformer designers is the failure of transformer due to internal and external faults. Among the various causes of failures in transformers, about 29% of failures are due to electrical disturbances [1].

Most of the electrical disturbances result in high currents through the windings. One of the most critical situations is due to external short circuit which produce very high winding currents resulting in high electromagnetic forces in the windings. The magnitude of the fault current depends upon the short circuit reactance of the transformer and the current increases to a maximum of 8 to 10 times the normal working current under short circuit fault. As the force created is proportional to the square of current, the electrical force can reach more than hundred times of normal electrical force under short circuit and also reaches its maximum within 0.01s [2].

The fault currents produce radial and axial component fluxes which interact with winding currents to produce axial and radial forces respectively. Depending on the distribution of forces and the mechanical integrity of the windings, the weakest winding region undergoes deformation. These forces not only displace/deform the windings [3] but also affect the other transformer components such as clamping ring, flitch plates and frames. Hence, it becomes necessary to calculate the intensity of short circuit and check the mechanical strength of structural parts under such conditions at the design stage itself [4].

This paper deals with the basic theory and calculation of electromagnetic force distribution and resulting displacement/deformation. Though analytical methods of calculating force and displacements are used widely, the exact distribution of force and displacement profile of the winding are successful with numerical methods for complex geometry with multiple materials. Finite Element method (FEM) based computation of force and displacement are carried out for cases from literature [5] and [6] for better understanding.

## II. ELECTROMAGNETIC FORCE

There are different types of faults which result in high over currents, viz. single line to ground fault, line to line fault with or without simultaneous ground fault and three phase fault with or without simultaneous ground fault. Usually the three phase symmetrical fault is the most severe one. Hence, it is usual to design a transformer to withstand a three phase short circuit at its terminals. Waters (1966) has discussed in detail about all the aspects of short circuit in transformers and calculations of all quantities like magnetic flux, flux density, force, etc. analytically and the same are referred in this section.

In general, the asymmetrical short circuit current ( $I_{sc}$ ) of a transformer for a three phase system is given by,

$$I_{sc} = \frac{1.8 \times \sqrt{2} \times S \times 10^6}{\sqrt{3} \times V \times z} \quad (A) \quad (1)$$

where  $I_{sc}$  - peak value of short-circuit current (A)

$S$  - rated output of transformer (MVA)

$V$  - rated line to line voltage (V)

$z$  - per unit impedance of the transformer

The current passing through a winding produce a magnetic flux which inturn along with the winding current produces axial and radial forces.

### A. Radial Force

In general, current through the concentric windings produce a magnetic flux as shown in Fig.1(a). Thus produced flux has two components viz. radial flux along radial direction and axial flux along the height of the winding. The axial flux interacts with the winding current and produces radial force ( $F_r$ ) as shown in Fig.1(b). Since the concentric windings, low voltage (LV) and high voltage (HV) windings carry currents in opposite directions, there is a large radial repulsive force between them, thus resulting in outward pressure on the outer

winding (HV) and a pressure towards the axis of the limb on the inner winding (LV).

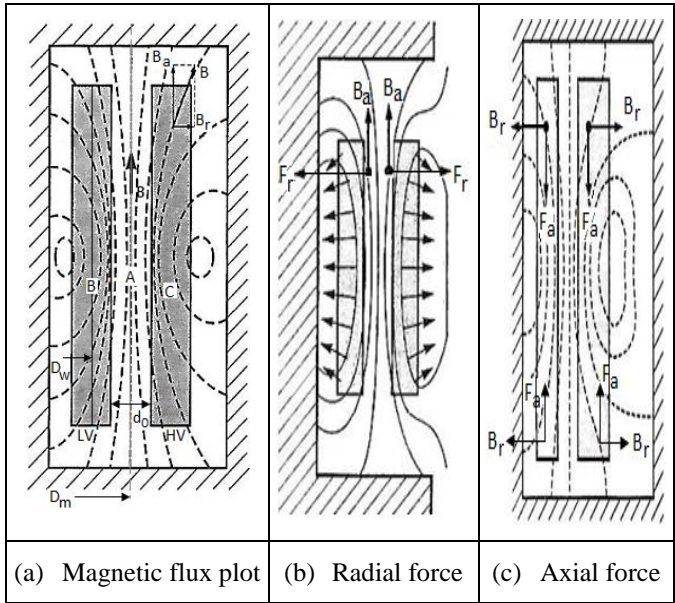


**Fig.1** Magnetic flux and the associated forces [7]

The axial component of the flux density ( $B_a$ ) at the center of the insulation in between the windings (at point A) is given by,

$$B_a = \frac{4 \times \pi \times (n.i)}{h \times 10^5} \quad (\text{T}) \quad (2)$$

and  $n.i$  - ampere turns (AT) of the winding  
 $h$  - length of the winding (cm)

$B_a$  – axial flux density in the duct at the mid point A (T)

The radial force ( $F_r$ ) at the point B (or C) is given by,

$$F_r = \frac{2 \times \pi^2 \times (n.i)^2 \times D_w}{h \times 10^7} \quad (\text{N}) \quad (3)$$

and  $D_w$  is the mean diameter of the outer winding (or inner winding).  $F_r$  is the outward force for outer winding and inward for the inner winding.

**B. Axial Force**

The radial flux interacts with the winding current and results in axial force ( $F_a$ ). As all discs of a winding carry current in the same direction, the axial force results in compression of the winding. For a uniform ampere-turn distribution in windings with equal heights, the axial forces at the winding ends are directed towards the winding center leading to compressive forces as shown in Fig.1(c). Even a small axial displacement of windings or misalignment of magnetic centers of windings can eventually cause enormous axial forces leading to failure of transformers.

The sum of axial forces ( $F_a$ ) at the middle of the winding is given by

$$F_a = \frac{2 \times \pi^2 \times (n.i)^2 \times D_m}{h^2 \times 10^7} \left[ d_0 + \frac{t_1 + t_2}{3} \right] (\text{N}) \quad (4)$$

and  $D_m$  - mean diameter of the duct between the windings (mm)  
 $d_0$  - duct width (mm)  
 $t_1$  and  $t_2$  - radial thickness of the LV and HV windings (mm)

Usually about 2/3 to 3/4 of the axial force is on the inner winding and about 1/3 to 1/4 is on the outer winding.

**III. WINDING DEFORMATION**

In general, winding deformation, displacement or damage of transformer windings occur due to mechanical and electrical faults due to various causes like,

- excessive mechanical force during a short circuit fault
- inter-turns short circuit as a result of lightning strokes
- due to ageing of paper, the insulation shrinks and the clamping pressure may be lost which reduces its voltage withstand strength
- vibration during transportation

In the present work, winding displacement/deformation due to short circuit current alone is considered. Due to the combination of axial and radial forces, the winding undergoes deformation as a result of displacements in both the radial and axial directions.

**A. Radial Deformation**

The radial deformation occurs in two ways. One is the forced buckling, that occurs when the inner winding is supported by spacers located in the axial direction and this happens when the stress value exceeds the material elastic limit as shown in Fig.2. The other strain is hoop buckling where the conductor is deformed in one or more radial points of the winding. The radial forces produced by the axial leakage field act outwards on the outer winding tending to stretch the winding conductor, producing a tensile stress (also called as hoop stress) as shown in Fig.3.

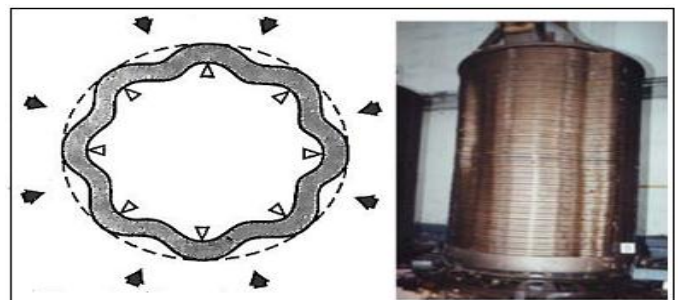


**Fig.2** Forced buckling [8]

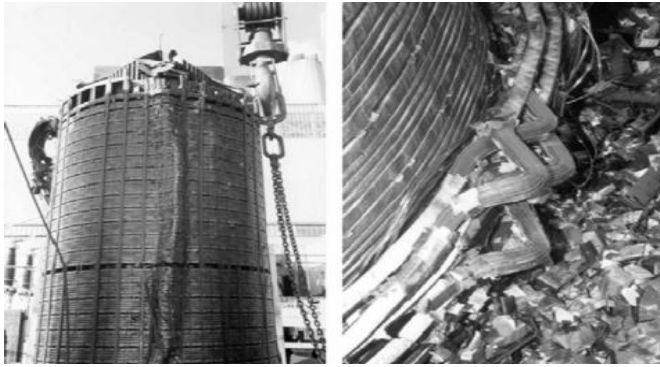


Fig.3 Hoop buckling in the outer winding [9]

B. Axial Deformation

Axial force is mainly directed away from the winding ends and towards the middle of the winding. So the highest compression occurs in the middle part of each winding. Fig.4 shows the bending of windings between supporting columns which can result in broken conductor insulation.

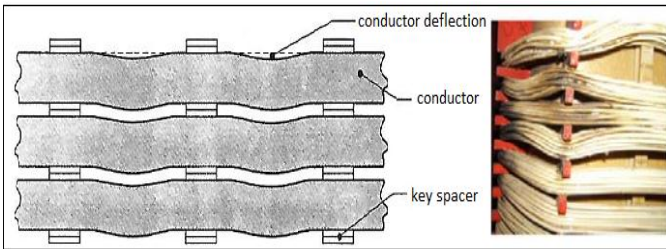


Fig.4 Axial bending of conductor between radial spacers [7]

When these axial forces are more than a certain limit, a failure can occur due to tilting of conductors in a zigzag way as shown in Fig.5. In this mode of failure, turning of conductor cross section occurs around the perpendicular axis of symmetry.



Fig.5 Tilting under an axial load [9]

IV. FORCE AND DISPLACEMENT USING FIELD EQUATIONS

To compute the distribution of axial and radial forces accurately, the actual configuration of the transformer need to be considered and computation can be effectively achieved by solving magnetostatic field equation numerically.

The electromagnetic force distribution in the windings is computed using Finite Element Method (FEM) based Magnetostatic field solver by using

$$\nabla \times \frac{1}{\mu}(\nabla \times \vec{A}) = \vec{J}_s \tag{5}$$

$$(\nabla \times \vec{A}) = \vec{B} \tag{6}$$

$$B_r = -\frac{\partial A_\phi}{\partial z}, \quad B_\phi = 0, \quad B_z = \frac{1}{r} \frac{\partial(rA_\phi)}{\partial r} \tag{7}$$

where  $\mu$  - magnetic permeability (H/m)

$A$  - magnetic vector potential (Wb/m)

$J_s$  - current density (A/m<sup>2</sup>)

$B_r, B_\phi,$  and  $B_z$  - directional components of the flux density in cylindrical coordinates (T)

The radial ( $B_r$ ) and axial ( $B_z$ ) components of the magnetic flux densities are computed using Equations (5), (6) and (7).

Electromagnetic forces ( $F$ ) produced due to winding current ( $i$ ) and the leakage flux density ( $B$ ) in the winding regions is given by the Lorentz force as,

$$d\vec{F} = i d\vec{l} \times \vec{B} \tag{8}$$

From the radial and axial components of flux densities, the axial ( $F_z$ ) and radial ( $F_r$ ) components of electromagnetic forces can be computed using Equation (9) as

$$\vec{F} = \int_v J_\phi \vec{\varphi} \times (B_r \vec{r} + B_z \vec{z}) dv = F_r \vec{r} + F_z \vec{z} \tag{9}$$

where  $J_\phi$  is the  $\phi$ -directional short-circuit current density and  $r, \phi$  and  $z$  are unit vectors in cylindrical coordinate and  $dv$  represents the incremental volume element.

Using the field approach, both the flux and force distribution can be estimated for the entire transformer which is essential for the prediction of the winding deformation profile. The mechanical deformation of the different parts of the transformer is computed using Coupled Magneto-Structural analysis.

The displacement ( $U$ ) of the winding is computed using

$$E A \nabla^2 U = -F \tag{10}$$

where  $F$  is the force,  $E$  is Young's modulus and  $A$  is the area of cross section.

V. FORCE DISTRIBUTION AND DEFORMATION OF COIL

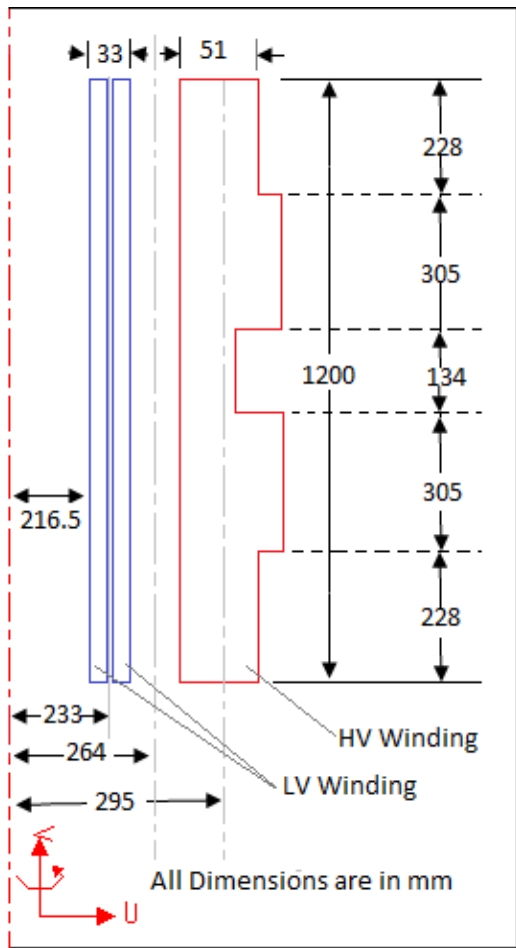
Short circuit events that occur in a network induce high mechanical forces in transformer windings. The withstand capability of the transformer under short circuit is a complicated one because of changes in electrical and mechanical parameters due to these forces. Hence, for better understanding of force and displacement computation and analysis in transformer windings, the work is started with case

studies from the literature using FEM based ANSYS Mechanical APDL Coupled Magneto-Structural solver.

**A. Short Circuit Force in A 5 MVA Transformer**

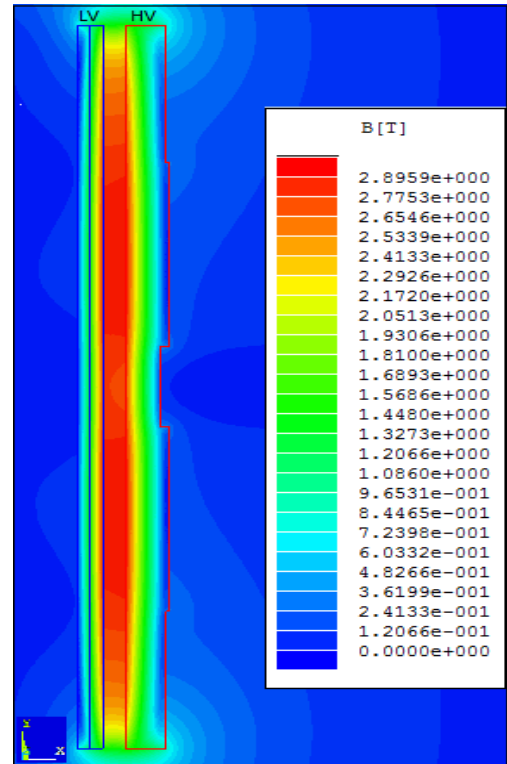
The distribution of electromagnetic forces in transformer windings under short circuit is computed and analysed using a two winding transformer. In this section, a 5 MVA, 22 kV/11 kV with concentric windings referred by Waters (1966) is considered and the same is shown in Fig.6. The outer winding (HV) is a disc winding with tappings and the inner winding (LV) is a two layer winding.

The LV and HV windings are energized with the short circuit current densities of  $67.27 \times 10^6 \text{ A/m}^2$  and  $45.1827 \times 10^6 \text{ A/m}^2$  respectively. The magnetic flux and the corresponding electromagnetic force distribution are computed in 2-D Axisymmetry using FEM based Coupled Magneto-Structural solver.



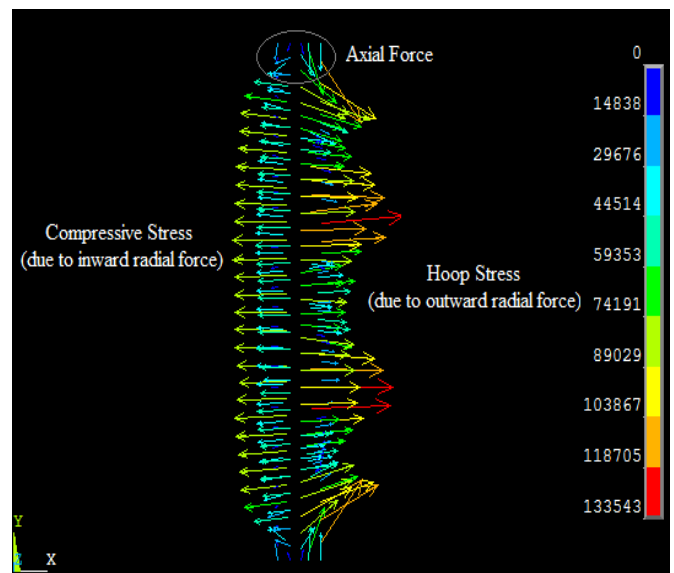
**Fig.6** Winding arrangement of the 5 MVA transformer

The magnetic flux density is found to be more in the duct between the windings and the maximum flux density occurs at the mid point of the duct (as shown in Fig.7) with the magnitude of 2.9 T and the same is 2.79 T when calculated analytically using Equation (2).



**Fig.7** Surface plot of magnetic flux density under short circuit

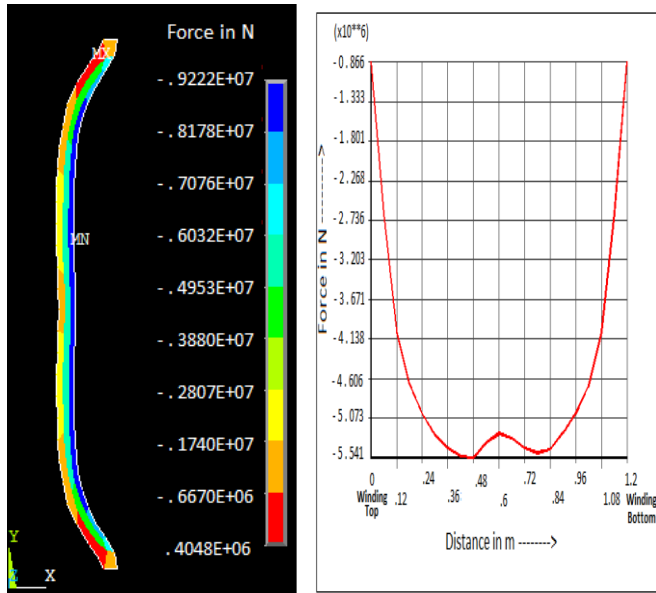
The electromagnetic force on the windings is computed using the flux distribution and the corresponding force vector plot is shown in Fig.8. It is observed from the figure that both the windings are subjected to both the axial and radial forces.



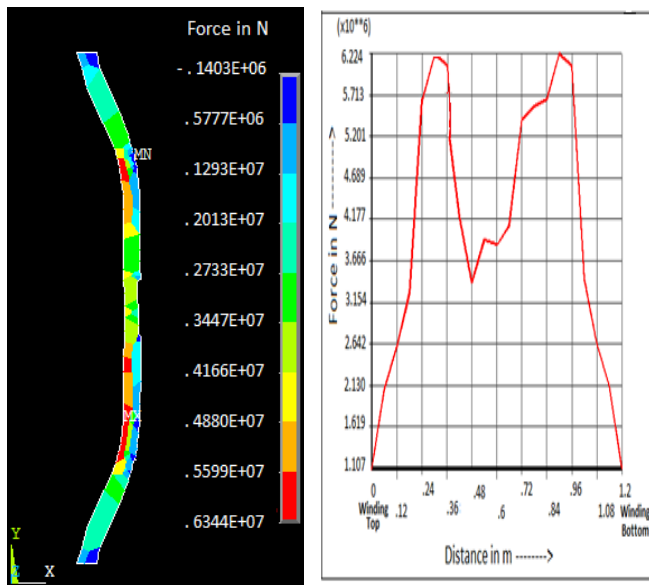
**Fig.8** Force vector plot

Fig.9 shows the radial force distribution along the LV and HV windings. Due to axial flux, a radial repulsive force between the inner and outer is produced. The radial force is minimum at the ends in both the windings and the maximum near the center for LV winding and near tappings for HV winding. The LV

winding experiences a buckling force acting inwards tending to crush or collapse the conductor and the HV winding experiences an outward force tending to stretch the conductor to produce hoop stress.

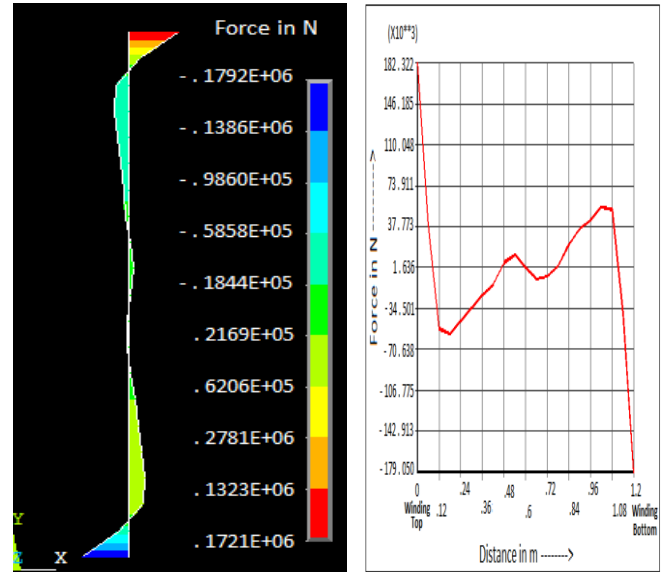


Surface plot of radial force      Radial force distribution  
**Fig.9(a)** Radial force distribution in LV winding

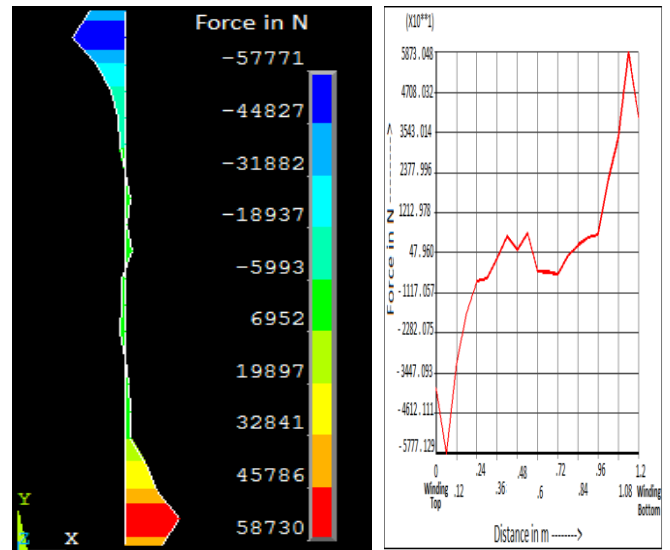


Surface plot of radial force      Radial force distribution  
**Fig.9(b)** Radial force distribution in HV winding

Due to radial flux, axial compressive force is produced on the windings and is found to be more near the winding ends and negligible at the centers as shown in the Fig.10. The maximum axial force in LV winding and is almost three times more than maximum axial force in HV winding.



Surface plot of axial force      Axial force distribution  
**Fig.10(a)** Axial force distribution in LV winding



Surface plot of axial force      Axial force distribution  
**Fig.10(b)** Axial Force distribution in HV winding

Table 1 gives the maximum values of forces in both the windings. 47% and 53 % of total radial forces act on LV and HV windings respectively. In case of axial force, 75% and 25% of total axial forces occur in LV and HV windings respectively agreeing well with Waters (1966).

The simulated values are compared with the analytically computed values (using Equation 3 and 4). Though not much differences are found between the numerically and analytically computed values in LV winding, due to the presence of tappings the percentage difference is found to more than 5% in HV winding. Thus, the methodology of force computation is verified with the literature and observed that the actual tapping configuration can be effectively incorporated in case of computation using FEM.

**Table 1.** Maximum force in LV and HV windings

Type of Force	Force (kN)	
	Simulated	Analytical (Waters 1966)
Radial force on LV	5541	5435
Radial force on HV	6224	6880
Axial force on LV	182	185
Axial force on HV	59	62

With the computed distribution of the forces and with the specified mechanical properties of the winding materials, the winding displacement profile can be estimated.

**B. Deformation of a Solenoid Coil**

To study the effect of force on windings, a solenoid coil used by Prakash Alapati & Kulkarni [6] is considered and is shown in Fig.11. The Copper coil is energized with a uniform current density of  $5 \times 10^6 \text{ A/m}^2$  and the deformation of the coil in a steady magnetic field is computed using Coupled Magneto-Structural formulation.

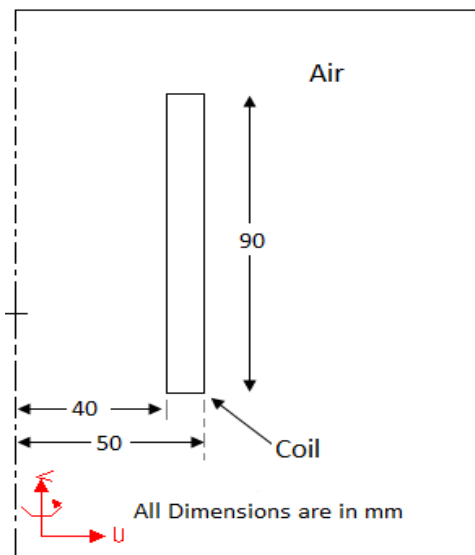
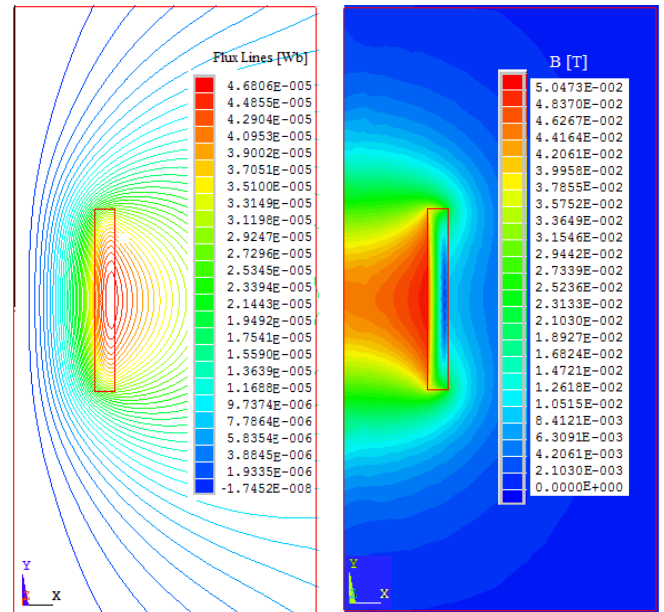


**Fig.11** Geometry of the solenoid coil

Fig.12 (a) and (b) show the magnetic flux and flux density plots. It is observed that the radial flux is maximum near the ends of the coil and the axial flux is maximum at the center of

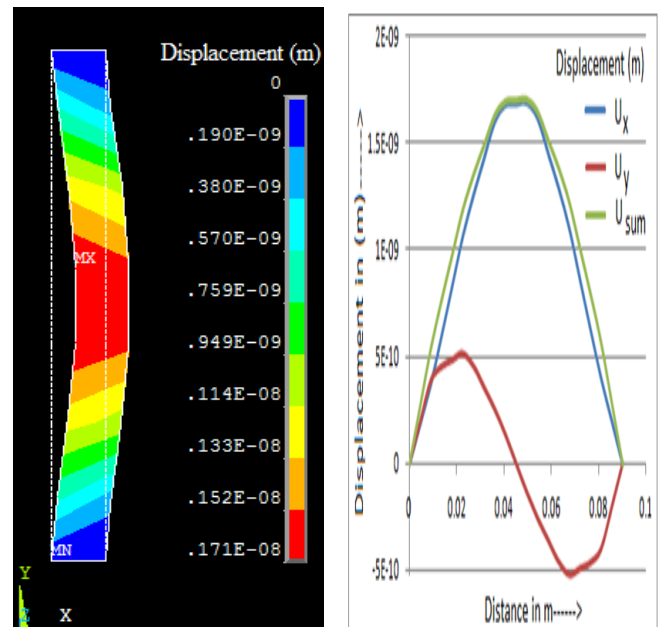
the coil which results in both radial (outward) and axial (compressive) forces.



(a) Magnetic flux lines (b) Surface plot of Magnetic flux density

**Fig.12** Magnetic Flux distribution in the solenoid coil

Fig.13(a) shows the deformed coil and Fig.13 (b) gives the displacements in both the axial ( $U_y$ ) and radial directions ( $U_x$ ). The coil undergoes a maximum deformation at the center with the radial outward displacement of  $1.71 \times 10^{-9}$  m, agreeing with the results of the literature with the percentage error of 3.7% .



(a) Surface plot of Deformation of the coil (b) Displacement profile

**Fig.13** Deformation of the coil

## VI. CONCLUSION

The computation of electromagnetic force distribution and the displacement profile using FEM based magneto structural field equations are discussed. In this work for better understanding typical examples from literature are considered.

- The magnetic flux and both the radial and axial force distributions due to short circuit in a two winding transformer is computed and analyzed using a 5 MVA, 22 kV/11 kV transformer and the following are observed here.
  - The maximum radial force occurs at the center of the LV winding and near the tappings in HV winding
  - The maximum axial force in LV winding is almost 3 times more than in HV winding
  - The difference in the maximum radial force computed using analytical equations and simulation ( FEM) is more due to the incorporation of the actual conductor geometry in the tappings of HV windings.
- The displacement profile due to magnetic flux and force distribution is computed and analyzed by using a solenoid coil and compared with the literature.

## REFERENCES

- [1] William, H & Bartley, PE 2000, 'Failure Analysis of Transformers', Proceedings of International Conference of Doble Clients.
- [2] Guo Zhenyan & Zhu Yinghao 2001, 'Short circuit mechanical force withstand ability test ', Proceedings of the Fifth International Conference on Electrical Machines and Systems, vol. 1, pp. 215-219.
- [3] Arul Sathya, M & Usa, S 2015, 'Prediction of Change in Equivalent Circuit Parameters of Transformer Winding Due to Axial Deformation using Sweep Frequency Response Analysis', accepted to publish in Journal of Electrical Engineering and Technology, pp. 30-36.
- [4] Du Shen-Hui & Zhu Wei-Lu 2009, 'Analysis of Short Circuit Axis-Direction Stability for Windings of Electrical Power Transformer', Power and Energy Engineering Conference, Asia-Pacific, pp. 1-4.
- [5] Waters , M 1966, 'The Short – Circuit Strength of Power Transformers', Macdonald & Co (Publishers) Ltd, Golf House, 2 Portman Street, London, W.1.
- [6] S.S. Prakash Alapati, S.V. Kulkarni, Coupled Magnetic -Structural Finite Element Analysis, Excerpt from the Proceedings of the COMSOL Conference 2009 Bangalore.
- [7] Giorgio Bertagnolli 2006, 'The ABB Approach to Short Circuit Duty of Power Transformers', June 2006.
- [8] Rosentino, AJP, Saraiva, E, Delaiba, AC, Guimaraes, R, Lynce, M, De Oliveira, JC, Fernandes, D & Neves W 2011, 'Modelling and Analysis of Electromechanical Stress in Transformers Caused by Short - Circuits', Renewable Energy and Power Quality Journal (RE&PQJ), ISSN 2172-038 X, no.9, Paper 432.
- [9] Cigre, WG A2.26 2008, 'Mechanica I-Condition Assessment of Transformer Windings using Frequency Response Analysis (FRA)', no. 342.